

modulation. For the modulation conditions used for Fig. 6, an effective line width of $\Delta B = 16$ G was calculated. Combining this with the known field gradient gives $\Delta z = 2.7$ μm , in good agreement with the experimental result. This spatial resolution is roughly an order of magnitude better than that obtained by conventional NMR imaging of nonmetallic solid samples (19).

The results presented in this report demonstrate that NMR force detection can achieve remarkable sensitivity and spatial resolution. Further advances are expected as progress is made toward more-sensitive cantilevers, higher field gradients, and lower temperatures. This work is also significant for the field of scanning probe microscopy. Previous scanning probes—including tunneling, atomic force, and near-field optical microscopies—have so far measured only the electronic properties of the sample. Now, we have shown that nuclear magnetism is also accessible.

REFERENCES AND NOTES

- J. A. Sidles, *Appl. Phys. Lett.* **58**, 2854 (1991).
- _____, *Phys. Rev. Lett.* **68**, 1124 (1992).
- _____, J. L. Garbini, G. P. Drobny, *Rev. Sci. Instrum.* **63**, 3881 (1992).
- D. Rugar, C. S. Yannoni, J. A. Sidles, *Nature* **360**, 563 (1992).
- O. Züger and D. Rugar, *Appl. Phys. Lett.* **63**, 2496 (1993).
- J. A. Sidles suggested cyclic adiabatic inversion as a means to create a slowly oscillating nuclear magnetic moment (personal communication).
- The processing steps for the fabrication of the cantilevers included (i) low-pressure chemical vapor deposition of silicon nitride onto (110)-oriented silicon substrates, (ii) patterning of the silicon nitride by photolithography and reactive ion etching, (iii) release of the cantilevers by KOH etching of the underlying silicon substrate, and (iv) critical point drying with high-pressure carbon dioxide. For further details, see S. Hoen *et al.*, in *Technical Digest of the 1994 Solid-State Sensor and Actuator Workshop*, Transducers Research Foundation, Hilton Head, SC, 13 to 19 June 1994 (in press).
- M. T. Rigglin, R. R. Knispel, M. M. Pintar, *J. Chem. Phys.* **56**, 2911 (1972).
- H.-M. Vieth *et al.*, in preparation.
- J. Mertz, O. Marti, J. Mlynek, *Appl. Phys. Lett.* **62**, 2344 (1993). In our case, damping feedback was implemented with a piezoelectric element attached to the cantilever holder. Unlike viscous damping, feedback-induced damping does not degrade the signal-to-noise ratio of the force detection.
- D. Rugar, H. J. Mamin, P. Guethner, *Appl. Phys. Lett.* **55**, 2588 (1989).
- T. R. Albrecht, P. Grütter, D. Rugar, D. P. E. Smith, *Ultramicroscopy* **42–44**, 1638 (1992).
- We define the force sensitivity, F_{rms} , as the rms amplitude of the sinusoidal force required to produce a dc signal level at the output of the lock-in amplifier equal to the rms noise at the lock-in output.
- Application note #3 on lock-in amplifier principles, Stanford Research Systems (Sunnyvale, CA).
- U. Dürrig, O. Züger, A. Stalder, *J. Appl. Phys.* **72**, 1778 (1992).
- A. Abragam, *The Principles of Nuclear Magnetism* (Oxford Univ. Press, London, 1961), pp. 86 and 545–548.
- C. P. Slichter, *Principles of Magnetic Resonance* (Springer-Verlag, Berlin, 1990), p. 24.
- The slight discrepancy between the experimental and theoretical results is attributable to the fact that part of the sample is off resonance because of the large field gradient and the finite thickness of the sample.
- For a review of solid-state NMR imaging, see, for example, D. G. Cory, in *Annual Reports on NMR Spectroscopy*, G. A. Webb, Ed. (Academic Press, London, 1992), vol. 24, pp. 87–180.
- We thank J. A. Sidles for many enlightening communications and for his suggestion of cyclic adia-

batic inversion. We also thank T. Albrecht, P. Grütter, D. P. E. Smith, and H. J. Mamin for their contributions to a previous version of the force detection apparatus. Some of the cantilever fabrication steps were performed at the Microfabrication Laboratory, University of California at Berkeley. The help of G. T. Mulhern with the critical point drying process was especially appreciated. O.Z. gratefully acknowledges financial support by the Swiss National Science Foundation.

27 January 1994; accepted 25 April 1994

Methane to Ethylene with 85 Percent Yield in a Gas Recycle Electrocatalytic Reactor-Separator

Y. Jiang, I. V. Yentekakis, C. G. Vayenas

Methane was oxidatively coupled to ethylene with an ethylene yield up to 85 percent and a total C_2 hydrocarbon yield up to 88 percent in a gas recycle high-temperature (800°C) electrocatalytic or catalytic reactor where the recycled gas passes continuously through a molecular sieve trap in the recycle loop. Oxygen is supplied either electrocatalytically by means of the solid electrolyte support of the silver-based catalyst or in the gas phase. The C_2 products are obtained by subsequent heating of the molecular sieve trap. The selectivity to ethylene is up to 88 percent for methane conversion up to 97 percent.

The oxidative dimerization, or “coupling,” of methane to the C_2 hydrocarbons ethane and ethylene with C_2 hydrocarbon yield Y_{C_2} in excess of 50% and ethylene yield $Y_{C_2H_4}$ higher than 40% has been a long-sought goal in heterogeneous catalysis (1–8). Achieving these threshold values is considered a necessary requirement for the development of an economically viable industrial process for the one-step production of ethylene from natural gas.

Since the seminal work of Keller and Bhasin (2), numerous catalysts have been found (3–9) that give selectivity to C_2 hydrocarbons (denoted by S_{C_2}) higher than 90% for low (<2%) methane conversion (hereafter denoted by C_{CH_4}). However, it was universally found (2–9) that the total C_2 hydrocarbon selectivity S_{C_2} and ethylene selectivity $S_{C_2H_4}$ decrease drastically with increasing conversion C_{CH_4} , so that Y_{C_2} (which equals $C_{CH_4}S_{C_2}$) and $Y_{C_2H_4}$ (equal to $C_{CH_4}S_{C_2H_4}$) are always less than 30% and 15%, respectively.

In a recent pioneering paper, Aris and co-workers (10) showed that Y_{C_2} and $Y_{C_2H_4}$ can be increased up to at least 50% and 17%, respectively, by using a Sm_2O_3 catalyst in a simulated countercurrent moving-bed chromatographic reactor (SCMBCR) to carry out the oxidative coupling of methane (OCM) reaction. In this reactor, the methane-oxygen feed is cycled periodically between four reactor units, maintained at a high (50:1) methane-to-oxygen ratio, and

four separating columns; the procedure is repeated indefinitely.

The reason for the low $S_{C_2H_4}$ and S_{C_2} values at high methane conversion C_{CH_4} and thus the reason for the low measured Y_{C_2} and $Y_{C_2H_4}$ values of earlier studies (2–9) is that the desired products ethylene and ethane are far more reactive with oxygen than with methane and therefore are easily oxidized to CO or CO_2 when their concentrations become comparable to that of methane (that is, for high methane conversion). Consequently, the observed improvement in C_2 yield (~50%) in the case of the SCMBCR (10) is attributable to the partial separation and removal of C_2 hydrocarbons from unreacted methane and oxygen. The same is predicted to apply for the countercurrent moving-bed chromatographic reactor (10).

We have almost entirely eliminated the problem of the high reactivity of the C_2 hydrocarbons during the OCM reaction by using a gas recycle reactor with a selective Ag-based OCM catalyst or electrocatalyst combined with an appropriate molecular sieve trap in the recycle loop (Linde molecular sieve 5A maintained at 30°C), which traps and thus protects an easily controllable percentage (up to 100%) of ethylene and of ethane produced during each gas cycle. An important feature of this molecular sieve material is that it traps ethylene much more effectively than ethane and thus leads to very high ethylene yields. In this way, we have obtained C_2 hydrocarbon yield values Y_{C_2} up to 88% and, more importantly, ethylene yield values $Y_{C_2H_4}$ up to 85%.

Department of Chemical Engineering, University of Patras, Patras GR-26500, Greece.

The catalytic or electrocatalytic, depending on the mode of oxygen addition, reactor consisted of an 8 mole percent Y_2O_3 -stabilized ZrO_2 (YSZ) tube (length, 15 cm; diameter, 2 cm) closed flat at one end and with an appropriately machined, water-cooled stainless steel reactor cap attached to the other end, thus allowing for continuous gas feed and removal (11, 12) (Fig. 1). Two types of catalyst films, which coated the inside walls of the YSZ tube, were tested and gave qualitatively similar results. One type was porous Ag (mass, 150 mg; superficial surface area, 10 cm^2) prepared by application of thin coatings of a Ag solution in butyl acetate, followed by drying and calcination as described elsewhere (12). The other type, of the same total mass and surface area, was a porous cermet consisting of 20% (by weight) Sm_2O_3 , doped with 1% CaO, and 80% Ag, which we prepared by thoroughly mixing the Sm_2O_3 (1% CaO) powder with the above Ag solution and then drying and calcining the mixture. The true surface area of both catalysts was estimated (12) to be

on the order of 500 cm^2 . Two similar Ag films deposited on the outside air-exposed walls of the YSZ tube acted as counter and reference electrodes (Fig. 1).

Constant currents I were applied with a galvanostat between the catalyst and the counter electrode. In this way, oxygen is supplied to the Ag-based catalyst at a rate $I/2F$ moles of atomic oxygen per second, where F is Faraday's constant, and the catalyst acts as an electrocatalyst (9, 11–13). Alternatively, oxygen was supplied to the gas phase through a needle valve. Appropriate setting of two needle valves (Fig. 1) allowed the reactor to be operated either as a batch recycle reactor (when repeated, batch operation can simulate continuous periodic unsteady-state performance) or as a continuous-flow steady-state recycle reactor.

The molecular sieve trap comprised one or two packed bed units in parallel, each containing 2 to 6 g of Linde 5A molecular sieve pellets (1.6 mm in diameter) maintained at 30°C . During repeated batch operation, the molecular sieve trap comprised

a single packed bed unit. At the end of each batch operation, the reactor was isolated with use of a bypass loop (Fig. 1), and the trap was heated to 400°C , thus releasing all the trapped ethylene, ethane, and CO_2 into the recirculating gas phase. By measuring the gas composition by on-line gas chromatography in the recycle loop (total volume, 50 cm^3), we could directly measure methane conversion C_{CH_4} , C_2 product selectiv-

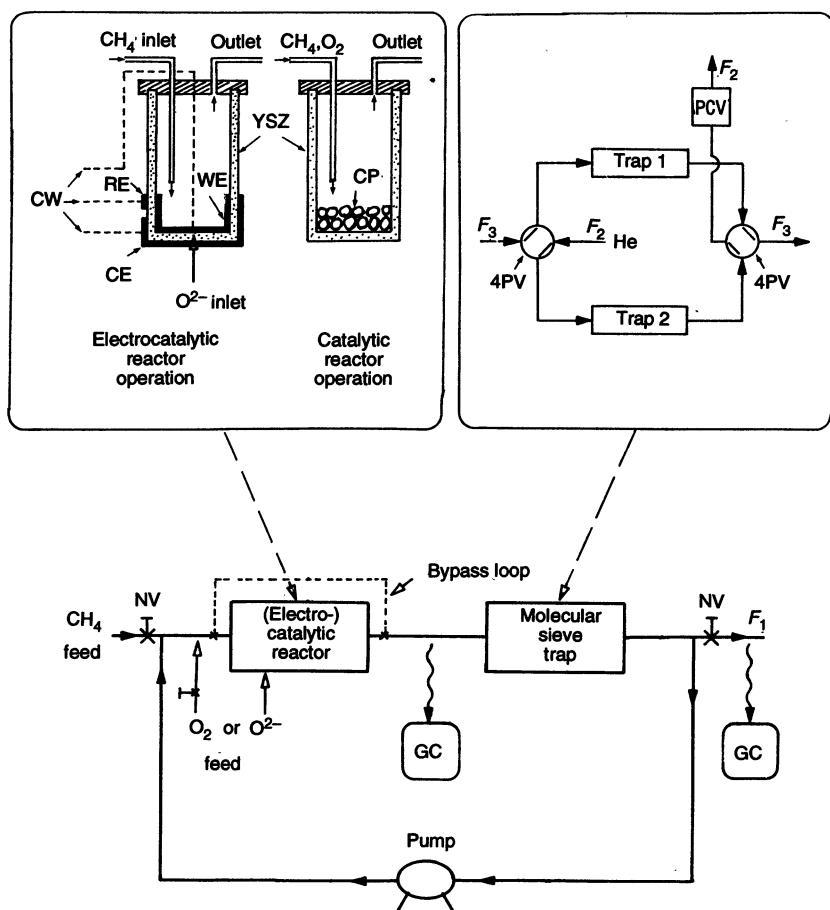


Fig. 1. Schematic of the gas recycle electrocatalytic or catalytic reactor-separator: WE, working electrode; CE, counter electrode; RE, reference electrode; CW, connecting wires; YSZ, yttria-stabilized zirconia solid electrolyte; CP, catalytic pellets; PCV, product collection vessel; 4PV, four-port valve; F_1 , exit flow rate; F_2 , product collection flow rate; F_3 , recycle flow rate; NV, needle valve; and GC, gas chromatograph.

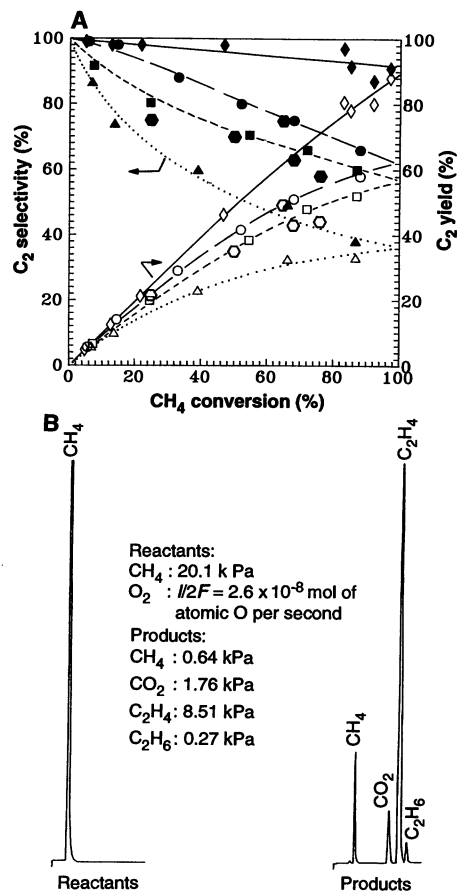


Fig. 2. (A) Effect of methane conversion and applied current on the selectivity (filled symbols) and yield (open symbols) of C_2 hydrocarbons. For continuous-flow steady-state reactor operation (hexagons), methane conversion was varied by fixing the applied current I and the exit flow rate F_1 : feed CH_4 partial pressure, 18 kPa in He; experiment performed at $I = 30, 5, 5, 7,$ and 9 mA and $F_1 = 3, 0.3, 0.2, 0.3,$ and $0.3\text{ cm}^3/\text{min}$ at standard temperature and pressure (STP), respectively, for the five points shown in order of increasing CH_4 conversion. For batch operation, methane conversion was controlled by varying the reactor operating time. The experiment was performed at various rates of atomic oxygen supply $I/2F$: $I = 5\text{ mA}$ (diamonds), 7 mA (circles), 15 mA (squares), and 30 mA (triangles). Initial CH_4 partial pressure = 20 kPa (20% CH_4 in He over Ag catalyst); $T = 835^\circ\text{C}$; adsorbent mass, 4 g; recirculation rate, $220\text{ cm}^3/\text{min}$ at STP. (B) Gas chromatogram of initial and final gaseous composition for the maximum C_2 yield point of (A); Porapak N column at $T = 80^\circ\text{C}$.

ity, and C_2 product yield. During continuous-flow steady-state reactor operation, the molecular sieve trap comprised two packed bed units in a swing-bed arrangement (Fig. 1); that is, one unit was maintained at 30°C to continuously trap the reactor products while the other was heated for 15 min to 400°C to release the products in a slow stream of He (typically at the same volumetric flow rate F_2 as the reactor exit flow rate F_1 to maintain a comparable level of dilution as in the reactor loop) flowing into a C_2 product collection vessel (Fig. 1). We used swing periods of 15 to 30 min, which led to a near steady-state level of C_2 hydrocarbons and CO_2 in the collection vessel exit, thus allowing for closure of the entire unit steady-state carbon mass balance. On-line analysis of the collection vessel was used to measure product selectivity, and methane conversion was measured in the recycle loop exit (Fig. 1).

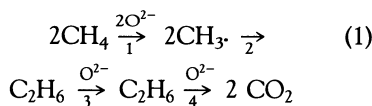
In both modes of operation, the total carbon mass balance closure was better than 5%. Oxygen conversion was complete. Ethylene, ethane, CO_2 , and H_2O were found to be the only detectable products. The molecular sieve traps were found to trap practically all ethylene, CO_2 , and H_2O produced; a significant percentage of ethane;

and practically no methane or oxygen.

For any fixed methane conversion, decreasing current in batch operation causes a pronounced increase in C_2 selectivity and C_2 yield (Fig. 2A). For $I = 5$ mA and 97% conversion, the C_2 selectivity is 91%, corresponding to a C_2 yield of 88%, which is the maximum C_2 yield obtained so far for the OCM reaction. We verified that batch operation can be repeated continuously by reloading the reactor without any loss in product selectivity or yield. Consequently, the batch mode results are also representative for repeated batch operation. Continuous-flow steady-state recycle reactor operation leads to selectivity qualitatively similar to that of batch operation (Fig. 2A). For $I = 5$ mA and 65% conversion, the C_2 selectivity is 76%, corresponding to a C_2 yield of 49%, which is significantly higher than previously reported values for continuous-flow steady-state reactor operation (2–9). For similar operating conditions, batch operation gives higher selectivity and yield values than continuous-flow steady-state operation (Fig. 2A). This is because, in the latter case, the methane concentration in the recycle loop is lower than the average methane concentration during each batch.

Figure 2B shows the gas chromatogram corresponding to the point of maximum C_2 yield of Fig. 2A. Not only is the C_2 hydrocarbon yield very high, but 97% of the C_2 hydrocarbon products is ethylene, which is by far more valuable than ethane.

In the same experiments the ethylene selectivity can increase with increasing methane conversion (Fig. 3A) because of the predominantly consecutive nature of the OCM reaction network



The molecular sieve adsorbent traps ethyl-

ene quantitatively, thus practically freezing step 4. Ethane trapping is only partial; thus, the desired step 3 is not decelerated significantly. Steps 1, 3, and 4 are predominantly catalytic or electrocatalytic, depending on the mode of operation, whereas step 2 is predominantly homogeneous, as established elegantly by Lunsford and co-workers (4, 8). To the best of our knowledge, the maximum ethylene yield of 85% (Fig. 3) is the highest reported for the OCM reaction. The observed dependence of S_{C_2} , $S_{C_2H_4}$, $S_{C_2H_6}$, Y_{C_2} , $Y_{C_2H_4}$, and $Y_{C_2H_6}$ on methane conversion (Fig. 3B) can be rationalized easily on the basis of the above consecutive reaction network.

The ethylene yield depends strongly on the amount of adsorbent for a given mass of catalyst and rate of oxygen supply $I/2F$, and for fixed methane conversion, there is an optimal amount of adsorbent for maximizing $Y_{C_2H_4}$ (Fig. 4). Excessive amounts of adsorbent cause quantitative trapping of ethane and thus a decrease in ethylene yield according to the above reaction network.

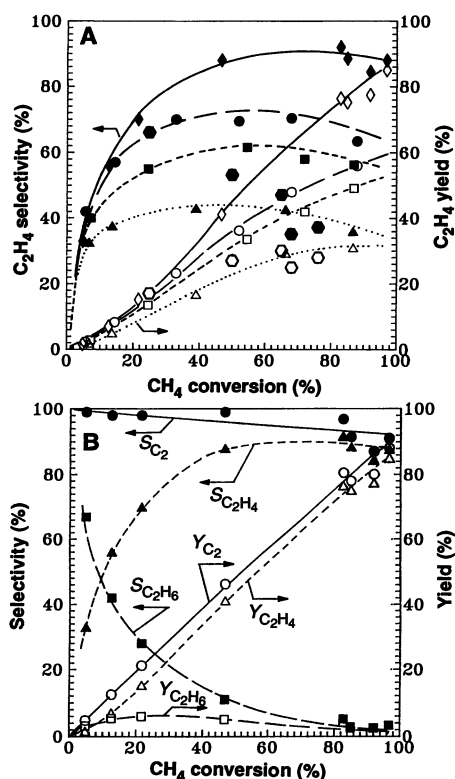


Fig. 3. (A) Effect of methane conversion and applied current on the selectivity and yield of ethylene. Symbols and conditions as in Fig. 2A. (B) Effect of methane conversion for $I = 5$ mA on ethylene, ethane, and total C_2 hydrocarbon selectivity and yield. Conditions as in Fig. 2A.

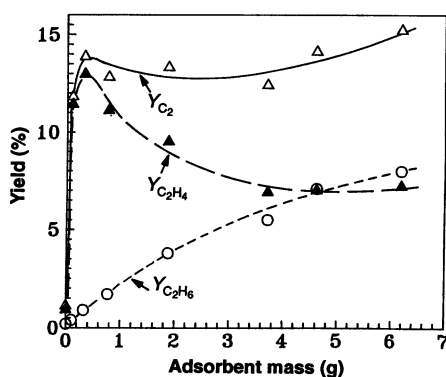


Fig. 4. Effect of adsorbent mass in the molecular sieve trap on ethylene, ethane, and C_2 hydrocarbon yield at fixed methane conversion $C_{CH_4} = 15\%$.

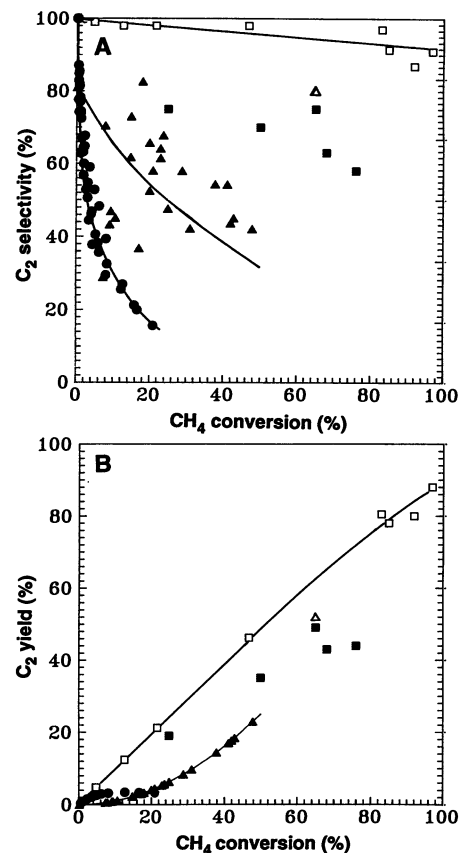


Fig. 5. Effect of methane conversion on (A) C_2 selectivity and (B) C_2 yield for some of the best state-of-the-art OCM catalysts (\blacktriangle) [from figure 5 of (5)], the simulated chromatographic reactor of Aris and co-workers (Δ) (10), and the present work, without (circles) and with (squares) gas recycling and C_2 trapping (open symbols, batch operation; filled symbols, continuous-flow steady-state operation).

A separate set of experiments in which oxygen was introduced to the gas phase at a rate comparable to $I/2F$, instead of electrochemically, gave practically the same results as those depicted in Figs. 2 to 4. Substituting Ag with the Sm_2O_3 -CaO-Ag cermet or substituting YSZ with α - Al_2O_3 as the cermet support gave only marginal differences with respect to the results presented in Figs. 2 to 4. Consequently, the amount of Sm_2O_3 added to Ag and the nature of the support do not play any important role in the observed behavior. Decreasing the gas recirculation flow rate from 220 to 50 cm^3/min at STP does not affect the reactor performance. By further lowering the recirculation flow rate, there is a gradual loss in C_2 and ethylene selectivity and yield.

The improvement in C_2 selectivity and yield of the present work is not attributable to the properties of the Ag catalyst, which is in fact inferior to most state-of-the-art catalysts and gives yields per pass less than 3% (Fig. 5), but is a result of the reactor design. Also, periodic unsteady-state reactor operation gives higher performance than steady-state reactor operation (Fig. 5), although industrial practice favors, in general, the latter mode of operation. Optimization could lead to further improvements in yields.

Our gas recycle reactor is simpler than and substantially different from the simulated countercurrent moving bed of Aris and co-workers (10) and has led to high values of C_2 yield and a pronounced enhancement in ethylene yield. The underlying idea is, however, very similar: protection of the highly reactive desired products by means of selective adsorption. The same type of reactor could also be used for other potential uses of methane, such as partial oxidation to methanol or formaldehyde (or both), by means of an appropriate choice of the catalytic and adsorbent material.

REFERENCES AND NOTES

1. L. L. Hegedus *et al.*, *Catalyst Design: Progress and Perspectives* (Wiley, New York, 1987), pp. 1–10.
2. G. E. Keller and M. M. Bhasin, *J. Catal.* **73**, 9 (1982).
3. W. Hinzen and M. Baerns, *Chem. Ztg.* **107**, 223 (1983).
4. T. Ito and J. H. Lunsford, *Nature* **314**, 721 (1985).
5. J. S. Lee and S. T. Oyama, *Catal. Rev. Sci. Eng.* **30**, 249 (1988).
6. K. Otsuka, K. Suga, I. Yamanaka, *Catal. Today* **6**, 587 (1990).
7. D. Eng and M. Stoukides, *Catal. Rev. Sci. Eng.* **33**, 375 (1991).
8. J. H. Lunsford, *Catal. Today* **6**, 235 (1990).
9. P. Tsiakaras and C. G. Vayenas, *J. Catal.* **144**, 333 (1993).
10. A. L. Tonkovich, R. W. Carr, R. Aris, *Science* **262**, 221 (1993), and references therein.
11. C. G. Vayenas, S. Bebelis, S. Ladas, *Nature* **343**, 625 (1990).

12. C. G. Vayenas, S. Bebelis, I. V. Yentekakis, H.-G. Lintz, *Catal. Today* **11**, 303 (1992).
13. C. G. Vayenas and R. D. Farr, *Science* **208**, 593 (1980).
14. We thank the EEC Joule Programme for partial

financial support, D. Sutija for preparing the Sm_2O_3 -CaO powder, and our reviewers for helpful suggestions.

8 February 1994; accepted 25 April 1994

Control of Structure and Growth of Polymorphic Crystalline Thin Films of Amphiphilic Molecules on Liquid Surfaces

Susan P. Weinbach, Kristian Kjaer, Wim G. Bouwman, Gerhard Grübel, Jean-François Legrand, Jens Als-Nielsen, Meir Lahav, Leslie Leiserowitz

The spontaneous formation and coexistence of crystalline polymorphic trilayer domains in amphiphilic films at air-liquid interfaces is demonstrated by grazing incidence synchrotron x-ray diffraction. These polymorphic crystallites may serve as models for the early stages of crystal nucleation and growth, helping to elucidate the manner in which additives influence the progress of crystal nucleation, growth, and polymorphism and suggesting ways of selectively generating and controlling multilayers on liquid surfaces. Auxiliary molecules have been designed to selectively inhibit development of the polymorphs, leading primarily to a single phase monolayer.

The ability to engineer three-dimensional (3D) crystals and crystalline thin films by control of polymorphism is important in applications ranging from the bioavailability of drugs to the design of materials for electronics. Such control requires an understanding of the mechanism by which molecules in a supersaturated solution assemble to form ordered aggregates or nuclei. Our knowledge of the structure and dynamics of such nuclei has, in general, been inferred from the structure of the observed crystals, which correspond to the thermodynamically most stable form or forms of the extended lattice (1). Additives may be designed to bind specifically to the surfaces of particular polymorphs and so inhibit their achieving the critical size for nucleation, allowing a desired phase to grow without competition. This method has been used for the separation of enantiomers by crystallization (1, 2) and for the growth of single crystals of metastable polymorphs, including polar crystals for nonlinear optics (3). Here we report the spontaneous formation of coexisting "polymorphic" trilayers and monolayers at the air-liquid interface and make use of auxiliary molecules to influence their thick-

ness and crystalline structure. These amphiphilic films, which can be directly monitored by grazing incidence x-ray diffraction (GID) (4–6) and specular x-ray reflectivity (6, 7), may serve as models for understanding the early stages of crystal nucleation and growth on the molecular level.

When spread on liquid water at surface pressure $\pi = 0$, arachidamide ($\text{C}_{19}\text{H}_{39}\text{CONH}_2$) forms a monolayer with the molecules tilted by about 18° from the normal to the liquid surface, with two molecules in a rectangular unit cell of dimensions $a = 4.69 \text{ \AA}$ and $b = 8.69 \text{ \AA}$ (8). When spread on formamide or formamide-water subphases, however, two trilayer phases are formed, with the relative ratio between them varying with time. The formation of multilayers and the coexistence of more than one crystalline form provide a system for study of the selective growth of crystallites at the liquid interface. We have therefore designed auxiliary molecules that may influence the mode of crystallinity.

The GID measurements were conducted on liquid surface diffractometers at the undulator beamlines BW1 at HASYLAB, Deutsches Elektronen-Synchrotron (DESY) (Hamburg, Germany) and Troika, European Synchrotron Radiation Facility (ESRF) (Grenoble, France). The amphiphiles (9) were spread at room temperature, with mean molecular area of 24 \AA^2 (calculated assuming coverage by a monolayer only) and $\pi = 0$, on the liquid surface in a Langmuir trough mounted on the diffractometer before the subphase was cooled to 5°C . In all systems, the molecules spontaneously formed highly crystalline films with corre-

S. P. Weinbach, M. Lahav, L. Leiserowitz, Department of Materials and Interfaces, Weizmann Institute of Science, 76100 Rehovot, Israel.

K. Kjaer and W. G. Bouwman, Physics Department, Risø National Laboratory, DK4000 Roskilde, Denmark. G. Grübel and J.-F. Legrand, Experiments Division, European Synchrotron Radiation Facility, Grenoble, France.

J. Als-Nielsen, Physics Department, Risø National Laboratory, DK4000 Roskilde, Denmark, and Experiments Division, European Synchrotron Radiation Facility, Grenoble, France.